Simulation of the Impedance Response of Thin Films as a Function of Film Conductivity and Thickness

Youngho Jin, Surajit Kumar and Rosario A. Gerhardt*
School of Materials Science and Engineering, Georgia Institute of Technology, Atlanta, GA 30332, USA
*Corresponding author: rosario.gerhardt@mse.gatech.edu

Abstract: Using parametric finite element simulations, film conductivities were varied in order to understand the role of film properties and geometry on nanoscale dielectric and spectroscopy measurements. The quasi-static forms of Maxwell's electromagnetic equations in time harmonic mode were solved using COMSOL Multiphysics® 4.4. The calculations were performed for a wide range of electrode size, film thickness and film conductivities to understand the interaction among these important parameters. Film and substrate interactions occurred in some cases. It is shown that equivalent circuit modelling can be used to describe the trends seen. This work highlights some of the factors that become important in the measurement and correct interpretation of dielectric properties of thin films and / or micro/nanoscale structures.

Keywords: COMSOL Multiphysics®, Thin film, Impedance spectroscopy, Dielectrics

1. Introduction

The dielectric properties of thin films are important in many different applications, such as microelectronics. Dielectric spectroscopy (also known as impedance spectroscopy) is one of the most common methods for measuring and studying the dielectric properties of thin films as a function of frequency. This method utilizes the interaction of an external ac electric field with the charge carriers and electric dipoles in the samples. A linear electrical response of a material is recorded by applying small electric signals. The lumped resistance and capacitance of the sample are estimated from the response. In recent years, the electrical characterization method is being extended to the nanometer scale range, thus high spatial resolution measurements of electrical properties have garnered great interest[1]. Currently, scanning probe microscopy based electrical measurement techniques, including nanoscale impedance microscopy(NIM)[2-4], electrostatic force microscopy(EFM)[5,6] and scanning capacitance microscopy(SCM)[7], have been used to probe electrical properties at the nanoscale. However, quantifying the dielectric properties using these techniques has been hampered by the size and the shape of the samples and the tips used to collect them[5]. The low micrometric tip-sample system forms a low capacitance in the range of a few fF (femto Farads). Such a low sample capacitance lowers the measurements resolution[8]. Recently, researchers have shown ways to overcome these problems using large tips and wear-resistant doped tips [5] or using half wavelength transformer connecting the conductive tip to a shunt resistor[9].

A systematic numerical study of film thickness, electrode size and substrate thickness, as well as film and substrate properties on the dielectric response is essential for furthering thin film science, nano-electronics and biomedical diagnostic applications. However, to the best of our knowledge, there have been no systematic studies of these effects on dielectric measurements, especially in the scanning probe microscopy based electrical measurement configurations. This paper addresses how film and substrate dielectric properties affect the impedance measurements of thin films.

The roles played by the measurement dependent parameters, such as the film thickness and electrode size, were investigated in an earlier study of insulating SiO_2 films deposited on a conductive substrate[10]. In this article, the measurement dependent parameters were evaluated further and the sample dependent parameters such as film conductivities were also varied while keeping the film thickness, contact size and substrate conductivity the same. Post processing was used to determine the related quantities, such as capacitance and resistance. A brief description of the simulation procedure is provided below. This work will help understand experimentally measured frequency dependent impedance data of thin films and the role played by the substrate on which the film is deposited.

Excerpt from the Proceedings of the 2015 COMSOL Conference in Boston

The finite element approach for evaluating impedance has been used by a few researchers to study a wide range of materials and various physical phenomena. However, the vast majority of impedance related works in the thin film area have been experimental, and simulation studies are very limited. Some numerical simulation works are listed below.

Ren and co-workers used a transmission line model to simulate the impedance of electroactive layers with non-uniform resistance and/or capacitance profiles[11]. Branković and co-workers developed a fractal model for simulating grain boundary regions of ceramic materials during impedance spectroscopy analysis[12]. Chen and coworkers have used the finite element method to simulate the effects of MIEC thin film electrodes for solid oxide fuel cells[13].

Using the finite element method in 2D, Fleig and co-workers calculated the impedance response of the effect of imperfect contacts between an electrode and a sample[14]. A 3D version of a similar work dealing with porous electrodes on electro-ceramics has also been published by the same authors[15]. They have also performed a 3D finite element analysis of highly resistive grain boundaries in the electroceramics[16]. In the latter article, the impedance spectra of polycrystalline samples with imperfect contact patterns have been calculated and analyzed.

In the current work we take a finite element approach to solve for the electric potential in a typical thin film electrical characterization configuration assuming isotropic and homogeneous properties of the thin films. The impedance and related quantities have been obtained by post processing the electric potential field.

2. Use of COMSOL Multiphysics®

In this section we provide a brief background on the simulation procedure of impedance measurements, which involve the polarization of dielectric materials under an applied electric field. A numerical calculation of the impedance, capacitance, and related quantities naturally requires the solution of the electric fields in the material under an applied electric potential or electric current. In the case of impedance measurements the potential/current is time varying and usually harmonic [17]. Impedance measurement setups involve small length scales (orders of mm) and low frequencies (Hz-MHz range). Hence, the electric field wavelength is typically several orders of magnitude larger than the dimensions of the sample that is measured. In such a situation the quasi-static approximation can be used [18].

Figures 1(a) and (b) show schematics of the cross sectional side view of the structures that have been simulated to calculate the impedance of thin films of varying conductivity deposited on a conductive substrate. Figure 1(a) shows three sub-domains: (1) the film thickness, t_{film}, electrical conductivity, σ_{film}, and electrical

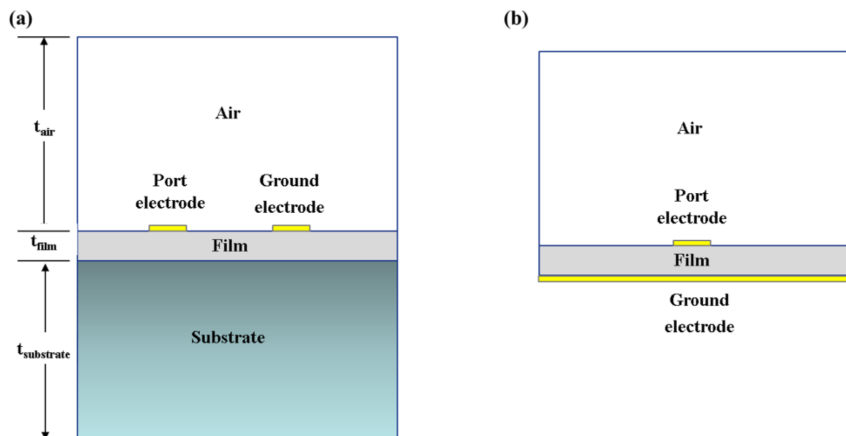

Figure 1. Schematics of the configuration used for impedance modeling, (a) side view of the 2D (full) model, and (b) side view f the 2D (simplified) model in which the substrate is ignored. (Modified from ref. [10].)

permittivity, ε_{film}; (2) the substrate with thickness, $t_{substrate}$, electrical conductivity, $\sigma_{substrate}$, and electrical permittivity, $\varepsilon_{substrate}$; and (3) air with thickness, t_{air}, electrical conductivity, σ_{air}, and electrical permittivity, ε_{air}. Figure 1(b) follows the same format except that no substrate is included. This simplified version of the thin film measurement ignores the substrate so that any possible interactions between thin film and the substrate can be excluded since only one electrode pad is simulated, while the ground electrode is actually placed on the bottom of the film, ignoring the substrate.

The surface electrodes, on which ac signals have been applied, have a width $d_{electrode}$. Because of the limitations of computational resources, 2D simulations have been used instead of full 3D. 3D simulations are computationally intensive when the film thickness is small or the contact electrode is small compared to the substrate thickness. The 2D full model displayed in Figure 1(a) was modified to have the substrate as a boundary condition of the bottom of a thin film, having the conductivity, permittivity and thickness of the real substrate. This modified 2D full model can further save computational resources, when the electron mobility is high due to high film conductivity.

In all cases, the electrode thickness can be ignored in the simulations because of the highly conductive nature of the electrode materials used in typical experimental measurements. Not incorporating the electrode thickness avoids the significant increase in the number of mesh elements that would be needed in the finite element model.

The simulations reported herein have been performed using the time harmonic-electric currents solver in the ac/dc module of COMSOL Multiphysics® Version 4.4 (*Comsol Inc.*, Burlington, MA), which implements a finite element method to solve partial differential equations. The objective was to solve the Maxwell's equation, as in equation (1), for the time harmonic electric potential phasor for 2D cases.

$$\nabla \cdot \left(\sigma + \varepsilon_r \varepsilon_0 \frac{\partial}{\partial t} \right) \cdot \nabla V = 0 \qquad (1)$$

The real and imaginary components of the lumped parameters of impedance (Z) or admittance (Y) at the port electrode have been calculated by using the built-in functions in COMSOL Multiphysics®. There are three different choices of ports and hence, three different ways of calculating the lumped parameters. The forced voltage port has been used in these calculations. In this method, voltage is applied to the port electrode, and the currents flowing through it are extracted. The total current flowing from the port electrode to the ground electrode is calculated by integrating the current density. Using these two quantities, admittance, Y, has been obtained. The lumped capacitance (C) can be calculated from Z or Y. Since C, Z, and Y are complex quantities, they have a real part (indicated by single primes) and an imaginary part (indicated by double primes). The following expressions show their interrelationships.

$$Z = \frac{1}{Y} = Z' + jZ'' \qquad (2)$$

$$C = C' + jC'' = \frac{Y''}{\omega} + j\frac{Y'}{\omega} \qquad (3)$$

Standard values of the dielectric constants of air (ε_{air} = 1.00059ε_0), SiO_2 (ε_{film} = 3.9ε_0) and Si ($\varepsilon_{substrate}$ = 11 ε_0) have been used in the simulations, where ε_0 is the permittivity of vacuum, 8.854×10^{-12} F/m. The conductivity of highly doped silicon ($\sigma_{substrate}$ = 100 S/m) was used as the substrate conductivity in the simulations. The air thickness above the film was 500 μm and the air conductivity was 10^{-14} S/m in the simulations. The film conductivities in the simulations have been varied from 10^{-1} S/m to 10^{-13} S/m. It has been assumed that the film and the substrate are homogeneous and have uniform dielectric properties.

3. Results

3.1. Effect of sample geometry using 2D simplified model

Table 1 and 2 show the effects of electrode size and film thickness on the calculated capacitance respectively using the simplified 2D model assuming a fully insulating film with conductivity σ_{film} = 10^{-13} S/m. These results are

Excerpt from the Proceedings of the 2015 COMSOL Conference in Boston

extensions of an earlier study[10], which have been expanded here to include larger film thickness and smaller electrode contacts.

Table 1 shows that as the electrode size increases, the accuracy of the simulation is improved. The difference in the capacitance calculated by the simulation and the capacitance calculated by a parallel plate capacitor formula can be very small when the electrode size is large. The error is as low as 0.02 % for a 3mm contact for a 100nm thick film. As shown in Figure 2, the electrical potential distribution near the electrodes expands more for a smaller electrode.

The effect of film thickness is presented in Table 2. It can be seen that the difference between the parallel plate model calculation and the COMSOL simulations can be quite large when the film thickness exceeds one micrometer at a constant 3 μm electrode size.

Table 1. Comparison of calculated capacitance using different circular electrode sizes.

Effects of electrode size (t_{film} : 100nm)			
$d_{electrode}$ (μm)	$C_{formula}$ (F)	$C_{simulation}$ (F)	Error (%)
3000	2.44 x 10^{-9}	2.44 x 10^{-9}	0.02
300	2.44 x 10^{-11}	2.45 x 10^{-11}	0.16
30	2.44 x 10^{-13}	2.48 x 10^{-13}	1.44
3	2.44 x 10^{-15}	2.73 x 10^{-15}	11.66

Table 2. Comparison of capacitance of 2D calculations using different film thickness.

Effects of film thickness ($d_{electrode}$: 3μm)			
t_{film} (nm)	$C_{formula}$ (F)	$C_{simulation}$ (F)	Error (%)
10000	2.44 x 10^{-17}	2.99 x 10^{-16}	839.54
1000	2.44 x 10^{-16}	4.78 x 10^{-16}	95.70
100	2.44 x 10^{-15}	2.76 x 10^{-15}	11.67
10	2.44 x 10^{-14}	2.48 x 10^{-14}	1.45

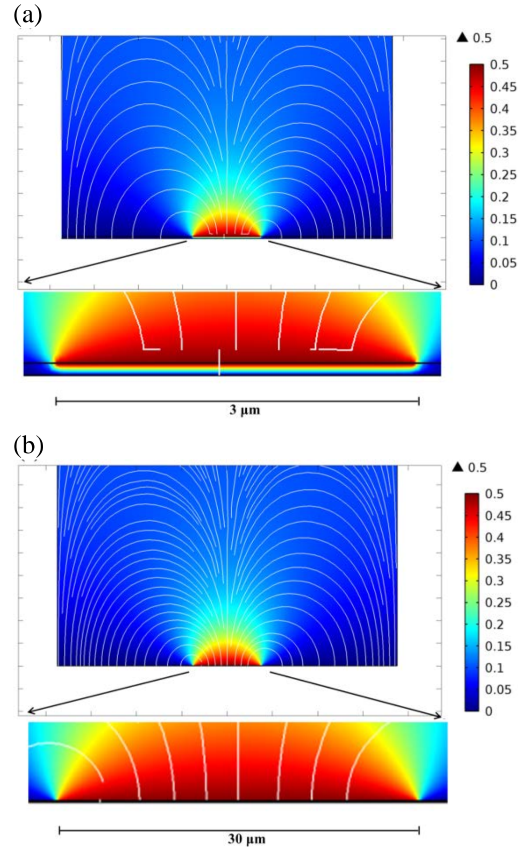

Figure 2. Electrode size effect on electric potential distribution using 2D (simplified) model. (a) $d_{electrode}$ = 3 μm and (b) $d_{electrode}$ = 30 μm at 1 Hz frequency. (σ_{film} = 100 S/m, t_{film} =100 nm)

3.2. Effect of film conductivity on the impedance response using the 2D full modified model

Figure 3 shows the impedance magnitude as a function of frequency for different film conductivities. When the film is very insulating, the impedance is very frequency dependent, but as the conductivity of the film increases, the frequency independent region grows wider until it shows no frequency dependence at all.

The phase angle plot as a function of frequency is displayed in Figure 4. The phase angle shows capacitive behavior ($\theta \rightarrow$ -90°) for films with very low conductivities while the behaviour is resistive ($\theta \rightarrow$ 0°) for films with very high conductivities. For intermediate conductivities, the behaviour is capacitive in the high frequencies and resistive in the low frequencies.

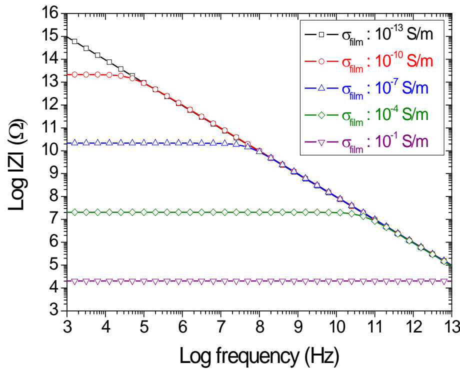

Figure 3. Bode plots for 2D (full modified) model showing impedance magnitude for several film conductivities when $\sigma_{substrate}$ = 100 S/m. (t_{film}=100 nm, $d_{electrode}$=3 µm)

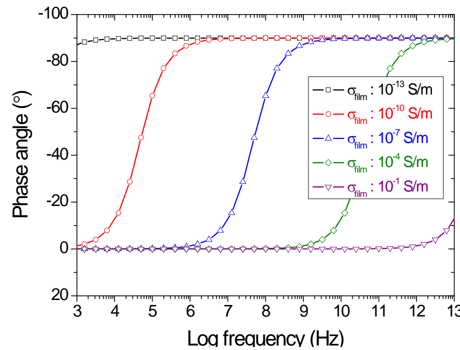

Figure 4. Bode plots for 2D (full modified) model showing phase angle for several film conductivities when $\sigma_{substrate}$ = 100 S/m. (t_{film}=100 nm, $d_{electrode}$ =3 µm)

3.3. Effect of film and substrate interactions

Figure 5 shows plots of real impedance Z' as a function of frequency for different film conductivities for the simplified 2D model that ignored the substrate effects. The curve is straight and frequency dependent for highly insulating films, while for the more conductive films the curves have straight line sections in the high frequency, then asymptotically merge into plateau regions in the low frequency.

In contrast, Figure 6 shows that the inclusion of the substrate properties, obtained using the modified 2D full model, results in markedly different behaviour for the plots of Z' as a function of frequency for the films with different conductivities. The differences in the plots are insignificant when the film conductivity was higher than 10^{-7} S/m.

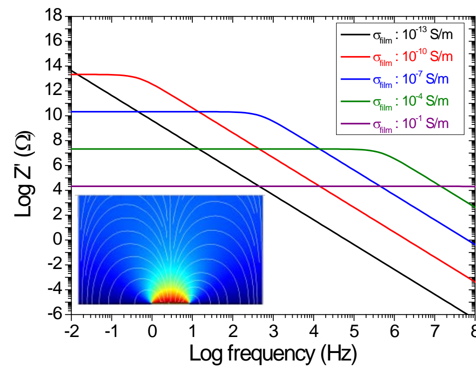

Figure 5. Bode plots for 2D (simplified) model showing real impedance for several film conductivities when the model does not include substrate effects. Inset shows the simulation configuration for a film with t_{film}=100 nm and $d_{electrode}$=3 µm.

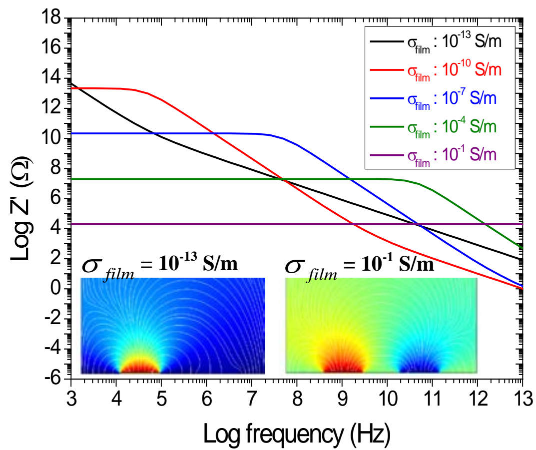

Figure 6. Bode plots for several film with different conductivities using the 2D (full modified) model that includes the substrate properties. These curves show that the real impedance can be substantially affected. Inset shows simulation configuration when t_{film}=100 nm and $d_{electrode}$=3 µm)

However, when the film conductivity was lower than 10^{-7} S/m, there was competition between the film and the substrate for the current flow resulting in a clearly deformed frequency response in the real impedance Z' versus log frequency curve as shown in Figure 6. This is most obvious for the cases where the conductivities of the film were 10^{-10} S/m and 10^{-13} S/m. These irregular responses have also been observed in other Bode plots (Y', M' and C'' plotted versus frequency, which are not shown in this paper).

3.4. Comparison of COMSOL simulations with equivalent circuit fitting

It is very useful to model the impedance response using an equivalent circuit model in order to evaluate the responses obtained [19]. In this way, one can have an idea as to how the conductive substrate affects the dielectric response of a given thin film configuration. Most materials can be modeled using a resistor and capacitor in parallel, therefore for the thin film configuration on top of a substrate, the equivalent circuit models will be made up of two parallel RC circuits that are connected in series.

Figure 7 depicts graphs for films with two different conductivities and shows the comparison between the numerical simulation via COMSOL and the equivalent circuit data fitting. It was found necessary to modify the capacitor and replace it with a CPE. The CPE can describe slight deviations from a perfect capacitor response. A CPE can be expressed by the following equation.

$$Z = 1/\,[Y_0(i\omega)^{\alpha}] \tag{4}$$

where the Y_0 is the constant and α is the CPE power index ($0\leq \alpha \leq 1$) if α is 1, Y_0 works as perfect capacitor.

A resistive current can be expected between the thin film and the substrate considering the conductive nature of the substrate. Figure 7 shows the presence of a slope change when film conductivity was 10^{-10} S/m. The equivalent circuit can precisely produce this slope change using 2 RC parallel circuits in series, which represent the response of the thin film and the substrate respectively.

Figure 8 shows C' bode plots of FEA simulation and equivalent circuit fitting for the same two films shown in Figure 7. The effects of conductive substrate are not detected in the real capacitance (C'), unlike the real impedance spectra shown in Figure 7. This illustrates that the irregular impedance response is related to the current flow between the film and the substrate and that real capacitance measurements are not highly affected by the substrate.

One can conclude that the dielectric responses of the thin film can be highly affected by the substrate when highly insulating thin films are deposited on a conductive substrate. However, the substrate conductivity does not appear to affect the real capacitance of the films.

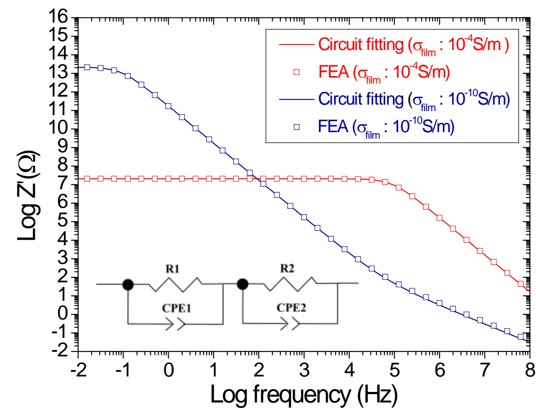

Figure 7. Bode plots for FEA 2D (full modified) model showing simulated real impedance as a function of frequency compared to the impedance calculated using equivalent circuit fitting for films with t_{film}=100 nm and $d_{electrode}$=3 μm.

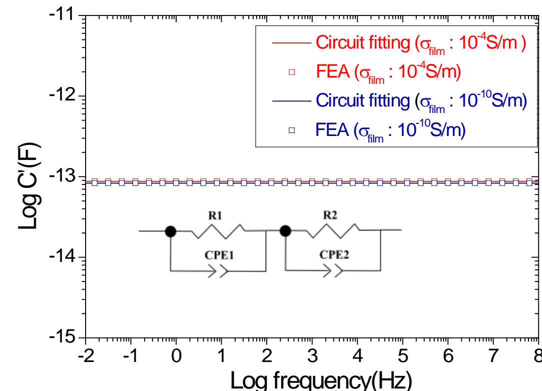

Figure 8. Bode plots for FEA 2D (full modified) model showing real capacitance compared to equivalent circuit fitting. (t_{film}=100 nm, $d_{electrode}$=3 μm)

4. Conclusions

This work highlights some of the factors that become important when conducting electrical measurements at the nano-scale. FEA simulations combined with equivalent circuit analysis can be used to obtain the correct interpretation of the electrical properties of thin films and micro / nanoscale structures.

5. References

1. O. Schneegans, P. Chrétien, F. Houzé, and R. Meyer, "Capacitance measurements on small parallel plate capacitors using nanoscale impedance microscopy," Applied Physics Letters, **90**, 043116 (2007)
2. L. Fumagalli, G. Ferrari, M. Sampietro, I. Casuso, E. Martinez, J. Samitier, et al., "Nanoscale capacitance imaging with attofarad resolution using ac current sensing atomic force microscopy," Nanotechnology, **17**, 4581 (2006)
3. L. Fumagalli, G. Ferrari, M. Sampietro, and G. Gomila, "Quantitative Nanoscale Dielectric Microscopy of Single-Layer Supported Biomembranes," Nano Letters, **9**, 1604-1608 (2009)
4. L. Fumagalli, G. Ferrari, M. Sampietro, and G. Gomila, "Dielectric-constant measurement of thin insulating films at low frequency by nanoscale capacitance microscopy," Applied Physics Letters, **91**, 243110 (2007)
5. L. Fumagalli, D. Esteban-Ferrer, A. Cuervo, J. L. Carrascosa, and G. Gomila, "Label-free identification of single dielectric nanoparticles and viruses with ultraweak polarization forces," Nat Mater, **11**, 808-816 (2012)
6. J. Waddell, R. Ou, C. J. Capozzi, S. Gupta, C. A. Parker, R. A. Gerhardt, et al., "Detection of percolating paths in polyhedral segregated network composites using electrostatic force microscopy and conductive atomic force microscopy," Applied Physics Letters, **95**, 233122 (2009)
7. P. J. Hansen, Y. E. Strausser, A. N. Erickson, E. J. Tarsa, P. Kozodoy, E. G. Brazel, et al., "Scanning capacitance microscopy imaging of threading dislocations in GaN films grown on (0001) sapphire by metalorganic chemical vapor deposition," Applied Physics Letters, **72**, 2247-2249 (1998)
8. G. Gramse, M. Kasper, L. Fumagalli, G. Gomila, P. Hinterdorfer, and F. Kienberger, "Calibrated complex impedance and permittivity measurements with scanning microwave microscopy," Nanotechnology, **25**, 145703 (2014)
9. H. Tanbakuchi, M. Richter, F. Kienberger, and H. Huber, "Nanoscale materials and device characterization via a scanning microwave microscope," in Microwaves, Communications, Antennas and Electronics Systems. COMCAS 2009. IEEE International Conference, 1-4 (2009)
10. S. Kumar and R. A. Gerhardt, "Role of geometric parameters in electrical measurements of insulating thin films deposited on a conductive substrate," Measurement Science and Technology, **23**, 035602 (2012)
11. X. Ren and P. G. Pickup, "Simulation and analysis of the impedance behaviour of electroactive layers with non-uniform conductivity and capacitance profiles," Electrochimica Acta, **46**, 4177-4183, (2001)
12. G. Branković, Z. Branković, V. Jović, and J. Varela, "Fractal Approach to ac Impedance Spectroscopy Studies of Ceramic Materials," Journal of Electroceramics, **7**, 89-94, (2001)
13. C. Chen, D. Chen, W. C. Chueh, and F. Ciucci, "Modeling the impedance response of mixed-conducting thin film electrodes," Physical Chemistry Chemical Physics, **16**, 11573-11583 (2014)
14. J. Fleig and J. Maier, "Finite element calculations of impedance effects at point contacts," Electrochimica Acta, **41**, 1003-1009 (1996)
15. J. Fleig and J. Maier, "The Influence of Laterally Inhomogeneous Contacts on the Impedance of Solid Materials: A Three-Dimensional Finite-Element Study," Journal of Electroceramics, **1**, 73-89 (1997)
16. J. Fleig and J. Maier, "The impedance of ceramics with highly resistive grain boundaries: validity and limits of the brick layer model," Journal of the European Ceramic Society, **19**, 693-696 (1999)
17. T. A. Davis, "Algorithm 832: UMFPACK V4.3---an unsymmetric-pattern multifrontal method," ACM Trans. Math. Softw., **30**, 196-199 (2004)
18. A. J. Lichtenberg, "The quasi-static approximation for moving and finite temperature plasmas," Electron Devices, IEEE Transactions on, **11**, 62-65 (1964)
19. E. Barsoukov and J.R. Macdonald, Impedance Spectroscopy: Theory, Experiment and Applications, John Wiley & Sons, 2005.

6. Acknowledgements

Research funding from the National Science Foundation (NSF) under DMR-1207323 is acknowledged and appreciated.